Activating the apelin receptor with LIT01-196, a metabolically stable apelin analog, reverses AVP-induced antidiuresis and hyponatremia

Adrien Flahault, Pierre-Emmanuel Girault-Sotias, Mathilde Keck, Rodrigo Alvear-Perez, Nadia de Mota, Lucie Estéoulle, Sridévi Ramanoudjame, Xavier Iturrioz, Dominique Bonnet, Catherine Llorens-Cortes

Title: Activating the apelin receptor with LIT01-196, a metabolically stable apelin analog, reverses AVP-induced antidiuresis and hyponatremia

Authors: Adrien Flahault[1*], Pierre-Emmanuel Girault-Sotias[1*], Mathilde Keck[1], Rodrigo Alvear-Perez[1], Nadia De Mota[1], Lucie Estéoulle[2], Sridévi M Ramanoudjame[2], Xavier Iturrioz[1], Dominique Bonnet[2,#], Catherine Llorens-Cortes[1,#]

Affiliations:

[1] Laboratory of Central Neuropeptides in the Regulation of Body Fluid Homeostasis and Cardiovascular Functions, Center for Interdisciplinary Research in Biology, INSERM, Unit U1050, Centre National de la Recherche Scientifique, Unite Mixte de Recherche 7241, Collège de France, Paris, France;

[2] Laboratory of Therapeutic Innovation, Unité Mixte de Recherche 7200, Centre National de la Recherche Scientifique, University of Strasbourg, Faculty of Pharmacy, Illkirch, France.

#To whom correspondence should be addressed: Catherine Llorens-Cortes. Laboratory of Central Neuropeptides in the Regulation of Body Fluid Homeostasis and Cardiovascular Functions, INSERM, U1050, Collège de France, 11 place Marcelin Berthelot, 75005 Paris, France. Tel: + 33 1 44271663. Fax: + 33 1 44271691. e-mail: c.llorens-cortes@college-de-france.fr and Dominique Bonnet Laboratory of Therapeutic Innovation, Unité Mixte de Recherche 7200, Faculty of Pharmacy, Illkirch, France, Tel: + 33 3 68854236, e-mail: dbonnet@unistra.fr

* Contributed equally and are both co-first authors

Abstract: Apelin and arginine-vasopressin (AVP) are conversely regulated by osmotic stimuli. Targeting the apelin receptor (apelin-R) to treat the Syndrome of Inappropriate Antidiuresis (SIAD), in which increased AVP secretion leads to hyponatremia, may be of interest. We previously developed LIT01-196, a metabolically stable apelin-17 analog, which behaves as a potent full agonist for the apelin-R. We show here that LIT01-196 has an *in vivo* half-life of 156 minutes in the bloodstream after subcutaneous (s.c.) administration in alert control rats. We demonstrate that LIT01-196 efficiently decreases the cAMP production induced in collecting ducts by dDAVP via AVP type 2 receptors (V2R). We also show in mouse cortical collecting duct cells that LIT01-196 reduces dDAVP-induced apical cell surface expression of phosphorylated aquaporin 2. This results in a LIT01-196-induced increase in aqueous diuresis in controls rats following s.c. administration, associated with a slight 11% increase in water intake and no alteration in renal function after 4 days of treatment. In a rat experimental model of AVP-induced hyponatremia, LIT01-196 s.c. administered (900 nmol/kg) for two days, blocked the antidiuretic effect of AVP and the AVP-induced increase in urinary osmolality highly efficiently, and induced a progressive correction of hyponatremia. These results demonstrate a major role of apelin, together with AVP, in the regulation of water balance, and suggest that apelin-R activation constitutes a new approach for hyponatremia treatment.

Introduction

Hyponatremia, defined in humans as a plasma sodium concentration below 135 mmol/l, is associated with various diseases, including chronic heart failure (CHF), liver cirrhosis, diuretic treatment and the Syndrome of Inappropriate Antidiuresis (SIAD) [1]. Hyponatremia is also associated with high mortality rates [2] in patients with liver failure [3], CHF [4] and chronic kidney disease [5].

Arginine-vasopressin (AVP or antidiuretic hormone, ADH) type 2 receptors (V2-R) are expressed in the kidney collecting ducts (CD). By acting on these receptors, AVP increases cAMP production, leading to the insertion of aquaporin-2 (AQP-2) into the apical membrane of CD, allowing water reabsorption and decreasing urine output (**Fig 1**) [6]. In SIAD, plasma AVP levels are inappropriately increased with respect to plasma osmolality [1]. V2-R antagonists, such as tolvaptan, block the stimulation of V2-R by AVP, and have been shown to correct hyponatremia efficiently in rodents [7] as well as in humans with SIAD [8–10]. Expected effects of aquaretic agents such as intense thirst, polyuria (24 h diuresis up to 6 L/day) and nocturia were observed [11]. Tolvaptan at the dose of 7.5 mg/day was also reported to carry a significant risk of overly rapid sodium correction, in 23 % of hyponatremia patients having baseline serum sodium concentration <125 mmol/l [12]. These patients exhibit the highest risk of developing osmotic demyelination syndrome when overly rapid correction of hyponatremia occurs [13,14]. Chronic treatment with V2-R antagonists has also shown efficacy in autosomal dominant polycystic kidney disease (ADPKD). However, aquaresis-related events led 8% of patients with ADPKD receiving tolvaptan to discontinue treatment [15]. Due to this concern and reports of hepatotoxicity associated with the chronic use of high tolvaptan doses[15–17], the development of new therapeutic

agents acting on new targets with a different mode of action could be useful for the treatment of disorders linked to excessive AVP secretion such hyponatremia and ADPKD.

Apelin is a neuro-vasoactive peptide identified as the endogenous ligand of the human orphan G protein–coupled receptor, APJ [18,19]. Following the identification of its endogenous ligand, this receptor was renamed the apelin receptor (apelin-R). Three molecular forms of apelin have been identified *in vivo,* apelin-36, apelin-17 (K17F) and the pyroglutamyl form of apelin-13 (pE13F) [20,21]. K17F has an affinity 16 times higher than that of pE13F for apelin-R (Ki, 0.05 nmol/l versus 0.8 nmol/l) but both peptides inhibit similarly forskolin-induced cAMP production in cells expressing the apelin-R. K17F is, however, 20 times more efficient than pE13F for inducing rat apelin-R internalization and β-arrestin mobilization [22,23]. Apelin and apelin-R [24,25] are expressed strongly in the supraoptic and paraventricular hypothalamic nuclei, in which double-labeling studies have shown them to colocalize with AVP in magnocellular vasopressinergic neurons [20,24–26]. The central administration of K17F in lactating rats, which display an increased phasic electrical activity of magnocellular vasopressinergic neurons and an increased AVP release from the posterior pituitary into the bloodstream, inhibits the activity of these neurons, leading to a decrease in circulating AVP levels and an increase in aqueous diuresis [20]. Apelin-R is also expressed in the kidney, both in the glomeruli and in all nephron segments including CD expressing AVP V2-Rs [27]. The intravenous injection of K17F into lactating rats by decreasing AVP-induced cAMP production, inhibits the AVP-induced AQP-2 insertion into the apical membrane of CD and increases aqueous diuresis [28]. These data were recently strengthened by the observation that apelin 13 decreases the phosphorylation and the apical membrane expression of AQP-2 in a highly differentiated mouse cortical CD cell line (mpkCCD) expressing the V2R and the ApelinR [29]. This suggests that the aquaretic effect of apelin is not only due to a central effect

involving an inhibition of AVP release into the bloodstream, but also to a direct renal effect in the CD, counteracting the antidiuretic effect of AVP mediated by V2Rs (**Fig. 1**) [30,31]. Furthermore, plasma AVP and apelin levels are conversely regulated by osmotic stimuli as well in rodents as in humans to maintain body fluid homeostasis [20,21,32]. In hyponatremia patients with SIAD [33], plasma copeptin levels (a biomarker of AVP release into the bloodstream in humans) are high and inappropriate for plasma sodium levels [33]. In addition, sex- and age-adjusted, plasma apelin concentrations were 26% higher in SIAD patients than in healthy subjects. Consequently, the balance between plasma apelin and AVP levels is not reached, as shown by the apelin to copeptin ratio as a function of natremia that was outside the 95% predicted physiological limits for plasma sodium in 86% of SIAD patients [33]. This imbalance contributes to the corresponding water metabolism defect in hyponatremia patients with SIAD (**Fig. 1**).

We therefore hypothesized that the supplementary activation of the apelin-R by a metabolically stable K17F analog could counteract AVP-induced water reabsorption and correct hyponatremia. Because the half-life of K17F is short (in the minute range *in vivo*), we generated LIT01-196 (**Fig. 2A**), a metabolically stable K17F analog, by adding a fluorocarbon chain to the N- terminal part of K17F, to increase its plasma half-life (> 24 h versus 4.6 min for K17F) [22]. LIT01-196 has a subnanomolar affinity for apelin-R and *in vitro* pharmacological profile similar to that of K17F [22]. In this study, we aimed (1) to determine the *in vivo* half-life of LIT01-196 in the blood circulation and its capacity to enter the brain following systemic administration, (2) to verify the efficiency of LIT01-196, as compared to K17F, to inhibit dDAVP-induced cAMP production in freshly microdissected CD (3) to define if LIT01-196 decreases the apical cell surface expression of phosphorylated aquaporin 2 (AQP-2) in mpkCCD cells (4) to determine the metabolic effects of LIT01-196 administered subcutaneously (s.c.) in alert rats and (4) to assess whether the

activation of apelin-R by LIT01-196 reversed AVP-induced antidiuresis and corrected hyponatremia in a rodent hyponatremic model, using tolvaptan as a reference aquaretic agent.

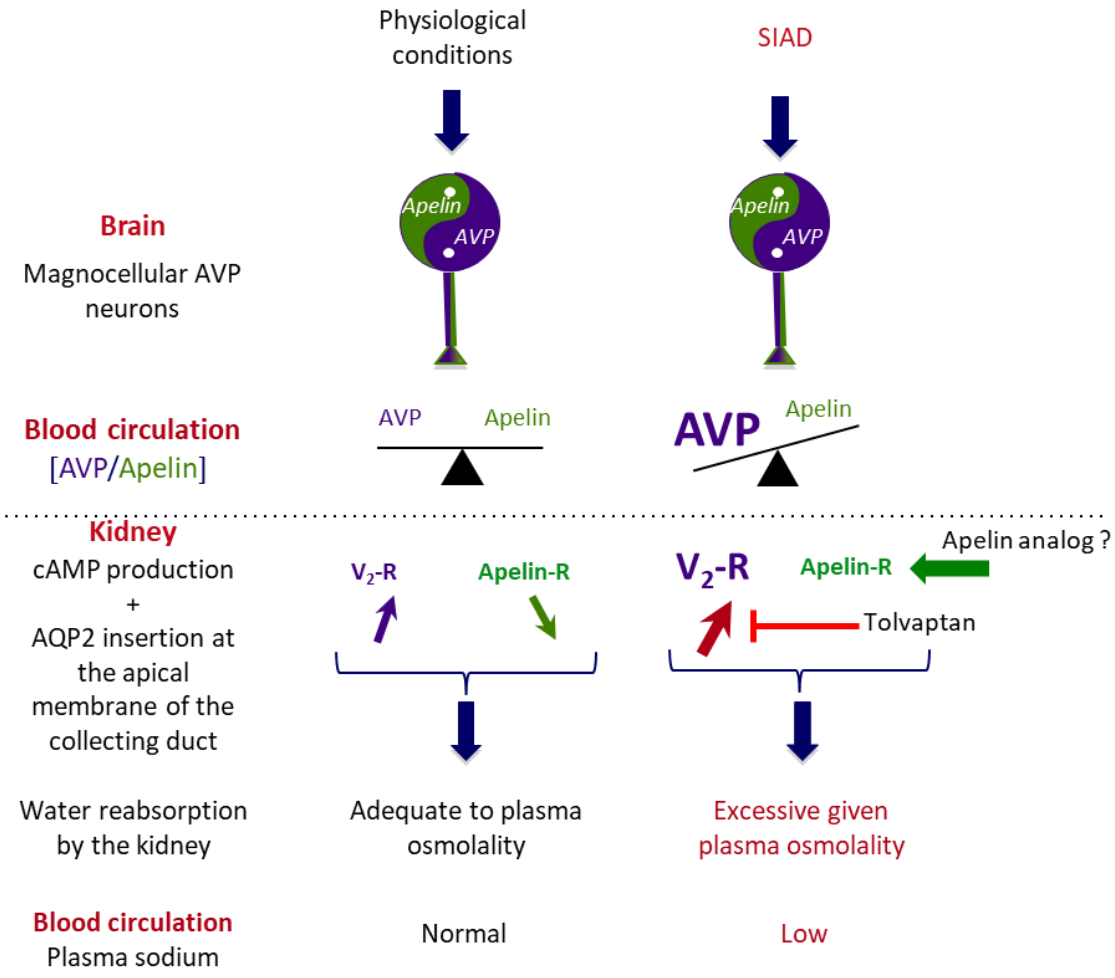

Fig. 1. Apelin and vasopressin regulation in physiological conditions and in SIAD. In physiological conditions, apelin and AVP are released in balanced proportions from the magnocellular AVP neurons, at levels appropriate for plasma osmolality. In the collecting duct of the kidney, AVP acts on V2-R, to increase cAMP production and aquaporin-2 (AQP-2) insertion, leading to water reabsorption. Conversely, apelin, through its action on apelin-R, has the opposite effect. In physiological conditions, water reabsorption is adequate and plasma sodium concentrations are normal. In SIAD, AVP release is excessive relative to plasma osmolality, leading to excessive water reabsorption by the kidney and hyponatremia. Tolvaptan blocks the effect of AVP on V2-R and corrects hyponatremia in SIAD. We hypothesize that the activation of apelin-R with a metabolically stable K17F analog, LIT01-196, would also correct

water homeostasis in this disease. Adapted from De Mota et al[20], Hus-Citharel et al[28] and Blanchard et al [33].

Materials and Methods

Study design

Sample size was determined before the study. For the hyponatremia study, the detection of a mean difference in plasma sodium concentration of 5 mmol/l (expected standard deviation of 3 mmol/l) between the treatment group and the control group would require the inclusion of at least 8 animals in each treatment group. AVP-treated animals with an insufficient antidiuretic response (urinary osmolality < 850 mOsm/kg) were excluded. The experimental design is described in **Fig. 4A**. AVP-treated animals were randomly assigned to treatment groups. Blinding was not feasible for treatment administration and sample collection, but the investigators were not aware of the treatment group during sample analysis. Each *in vitro* experiment was performed at least three times in triplicate.

Drugs, antibodies and reagents

K17F was synthesized by PolyPeptide Laboratories (Strasbourg, France). AVP and (Deamino-Cys^{1},D-Arg^{8})-vasopressin (dDAVP) were obtained from Bachem (Bubendorf, Switzerland). Tolvaptan was obtained from Activate Scientific (Prien, Germany). LIT01-196 (300 mg) was synthesized by the *Laboratoire d'Innovation Thérapeutique* (CNRS UMR7200, Illkirch, France as previously described [22]. [^{125}I]-pE13F (monoiodinated on Lys^{8} with Bolton-Hunter reagent) and [^{125}I]-(Tyr2Arg8)-AVP were purchased from PerkinElmer (Wellesley, MA, USA). A specific AVP-[Arg8] Ab was obtained from Peninsula Laboratories International (San Carlo, CA, USA), and rabbit polyclonal antibodies directed against the apelin fragment K17F were produced in the laboratory, as previously described [24]. Sodium heparinate, lithium heparinate and EDTA were obtained from SIGMA-ALDRICH (Saint-Quentin Fallavier, France). Isoflurane

(Isovet) and meloxicam (Metacam) were obtained from Centravet (Nancy, France). Drugs administered s.c. were diluted in 0.9% NaCl (saline, 1 ml/kg) for injection, except for tolvaptan, which was administered in 100% DMSO (0.2 ml/kg) due to its poor solubility in water.

Animals

Swiss mice (25-30 g) and male Sprague Dawley rats (210-230g) were obtained from Charles River Laboratories (L'Arbresle, France). Whilst housed in our animal facility, they were given free access to normal chow and water, and they were maintained under 12-h light/dark cycles throughout the study. When required for i.v. administration, a right femoral venous catheter was implanted in the rats, by tunneling under the skin, under isoflurane anesthesia (4% for induction, 2% for maintenance). Meloxicam (Metacam) was administered postoperatively (1 mg/kg s.c.) for analgesia. All experiments were carried out in accordance with current international guidelines for the care and use of experimental animals, and the experimental protocols were approved by the national animal ethics committee (CEEA, reference numbers 2016-10#3672, 2017-01 #7844 and 01966.02) and ethics regional committee for animal experimentation in Strasbourg (APAFIS reference number 1341#2015080309399690).

Cell line sources and culture conditions

CHO-K1 cells were obtained from American Type Culture Collection, Rockville, MD, USA and were maintained in Ham's F12 medium supplemented with 10% fetal calf serum, 0.5 mmol/l glutamine, 100 units/ml penicillin and 100 µg/ml streptomycin. HEK-293T cells were obtained from Cancer Research UK, London Research institute and were grown in DMEM medium supplemented with 10% fetal calf serum, 0.5 mmol/l glutamine, 100 units/ml penicillin and 100 µg/ml streptomycin. A highly differentiated murine renal cortical collecting duct principal cell (CCD) line, mpkCCDcl4[34], which has retained the main characteristics of the parental CCDs

from which they were derived[35]. This cell line was provided by Dr Michel-Robert Popoff from the Pasteur Institute who previously performed studies on these cells[36]. mpkCCD cells were grown in 1:1 (vol/vol) Ham's F12 : DMEM medium supplemented with 2% fetal calf serum, 20 mmol/l D-Glucose, 20 mmol/l Hepes, 1 % penicillin/streptomycin, 5 µg/ml insulin, 50 nmol/l dexamethasone, 60 nmol/l sodium selenate, 1 nmol/l triiodothyronine, 10 ng/ml d'EGF and 5 µg/ml transferrin.

Microdissection of rat outer medullary collecting ducts

The left kidney of male rats was prepared for nephron microdissection, as previously described [37]. Pieces of outer medullary collecting ducts were isolated under a stereomicroscope.

Membrane preparations and radioligand binding experiments.

Membranes from CHO cells stably expressing rat ApelinR-EGFP were prepared as previously described [23]. We compared the affinities of K17F and the new batch of LIT01-196 by performing classical binding studies with pE13F (Bolton-Hunter radioiodinated on the lysine residue in position 8) as the radioligand. Briefly, membrane preparations (0.5–1 µg total mass of membrane protein/assay) were incubated for 1 h at 20°C with 20 nmol/l [^{125}I]pE13F in binding buffer alone (50 mmol/l Hepes, 5 mmol/l $MgCl_2$, 1% BSA, pH 7.4) or in the presence of pE13F, K17F or LIT01-196 at various concentrations (0.01 pmol/l to 100 µmol/l). The reaction was stopped by adding ice-cold binding buffer and filtering through Whatman GF/C filters. The filters were washed and radioactivity was counted with a Wizard 1470 Wallac gamma counter (Perkin Elmer, Turku, Finland).

cAMP assay.

cAMP assays are described in the Supplementary Materials and Methods.

Measurement of phosphorylated AQP-2 immunoreactivity in mpkCCD cells treated by dDAVP, dDAVP +K17F or dDAVP + LIT

mpkCCD cells were seeded in 12 mm Transwell filters of 0.4 µm pore size at a density of 160, 000 cells/cm^2 and were grown for 5 days. Twenty-four hours before the experiment cells were starved with depletion media (1:1 (vol/vol) Ham's F12 : DMEM medium). Then, cells were treated at the basolateral compartment with depletion media (vehicle) or with 10 nmol/l of dDAVP in the presence or in the absence of 10 µmol/l K17F or LIT01-196 for 1h at 37 °C. Cell culture medium was removed and cells were fixed with 4% formaldehyde in PBS1X for 10 min at 4°C, and permeabilized with PBSTriton X-100 0.5% for 5 min at 20 °C. Then, inserts were incubated in 5% PBS-BSA for 60 min at 20°C to block non-specific protein binding. Inserts were subjected to immunostaining with a rabbit anti-AQP-2-pS269 antibody (1/200, Cliniscience, France) and a mouse monoclonal anti-occludin antibody (1/200, Santa Cruz, Cliniscience, France) for 16 hours at 4°C. Inserts were then incubated with goat anti-rabbit Alexa Fluor Plus 647 or goat anti-mouse Alexa Fluor plus 488 secondary antibodies (Invitrogen) for 60 min at 20°C. Inserts were detached and mounted onto microscopy slides with Pro Long Aquafade containing DAPI (Invitrogen). Slides were analyzed in the x-y and x-z axes under a 63x/1.4 Oil WD: 0.17 mm objective with a Zeiss Axioobserver Z1 inverted spinning-disk microscope equipped with a camera sCMOS Hamamatsu 2048*2048 / pixel size : 6.45*6.45 µm and the lasers (405 nm; 100mW, 491 nm; 150mW and 642 nm; 100mW). Microscope settings were identical for all the samples and experiments were randomized and blinded.

Apelin and AVP radioimmunoassays

The radioimmunoassays are described in the Supplementary Materials and Methods.

Plasma LIT01-196 measurement by mass spectrometry analysis

The mass spectrometry analysis is described in the Supplementary Materials and Methods**.**

Plasma protein binding of LIT01-196

Plasma protein binding of LIT01-196 is described in the Supplementary Materials and Methods**.**

AVP-induced hyponatremia

Hyponatremia was induced in male Sprague Dawley rats with an osmotic minipump (ALZET 2001, 200 µl, flow rate of 1 µl/h for 7 days), obtained from Durect Corporation (Cupertino, CA, USA) and filled with a solution of saline and AVP (at various concentrations), which was implanted subcutaneously under isoflurane anesthesia. Meloxicam was administered postoperatively for analgesia. Animals were then individually housed in metabolic cages (Techniplast), and given a semi-liquid diet consisting of 25 ml GelDiet Breeding-10 (SAFE, Augy, France) mixed with 25 ml tap water/day, with water available ad libitum. Animal weight, water and food consumption were measured daily. Urine was collected daily, urinary electrolytes (Na^+,K^+,Cl^-) were determined with an ISE 3000 (Caretium Medical Instruments, Shenzhen, China) and urinary osmolality was measured with a Cryobasic 1 osmometer (Astori Tecnica, Poncarale, Italy). Blood samples were collected on ice, before implantation of the osmotic minipump, and before drug administration, under isoflurane anesthesia, from the tail vain (4 µl of lithium heparinate (1600 IU/ml) for 400 µl of blood). The blood samples were immediately centrifuged (4°C, 2600 x g, 20 min), and plasma electrolyte (Na^+,K^+,Cl^-) levels were quantified with an ISE 3000. On the last day of the experiment, blood was also collected on ice by intracardiac puncture. This blood sample was collected into lithium heparinate under isoflurane anesthesia; plasma electrolyte levels were determined as described above and the animals were immediately killed by carbon monoxide inhalation. The experimental protocol is summarized in **Fig. 4A**.

Plasma glucose levels and fractional excretion of water and sodium

Fractional excretion of water (in %) was calculated using the following formula: (plasma creatinine / urine creatinine) x100. Fractional excretion of sodium (in %) was calculated using the following formula: (plasma creatinine x urine sodium / urine creatinine x plasma sodium) x 100. Blood and urine creatinine, urea nitrogen and glucose levels were determined using an AU5800 Beckman Coulter chemistry analyzer (Beckman Coulter, Villepinte, France).

Histological analyzes

Histological analyzes methods are described in the Supplementary Materials and Methods.

Blood pressure measurements

Blood pressure measurements are described in the Supplementary Materials and Methods.

Echocardiographic measurements

Left ventricular ejection fraction was determined in mice under isoflurane anesthesia at baseline and 3 hours after s.c. administration of the compound, as previously described[38].

Statistical analysis

We used Mann-Whitney U tests or paired Wilcoxon tests for comparisons between two groups, and ANOVA or Kruskal-Wallis tests followed by post-hoc comparisons for comparisons between multiple groups, when appropriate. We used a linear mixed-effects model to compare repeated values recorded over time, with time, treatment group and the measured parameter as fixed effects and the unique animal identification number as a random effect. We assessed the effects of treatment by performing an analysis restricted to measurements taken after treatment administration. The normality of the data was assessed visually and with the Shapiro-Wilk normality test. The data represented are means, with error bars to indicate the standard error of

261 the mean. The number of experiments or animals used is indicated in each figure legend.
262 Statistical analysis was performed with R software version 3.4.3 [39].
263

Results

Ability of LIT01-196 to bind and activate ApelinR

We first evaluated the ability of the new batch of LIT01-196 (300 mg), synthesized in large quantities for *in* vivo experiments, to bind to apelin-R and to inhibit forskolin-induced cAMP production in CHO cells stably expressing rat apelin-R-EGFP. As previously reported [22], LIT01-196, like K17F, bound to rat apelin-R with an affinity in the subnanomolar range (K_i values for K17F and LIT01-196 of 0.14 ± 0.02 and 0.34 ± 0.05 nmol/l, respectively) (**Fig. S1A**). In CHO cells stably expressing apelin-R-EGFP, LIT01-196 inhibited the cAMP production induced by 5 µmol/l forskolin with an IC_{50} of 1.7 ± 0.5 nmol/l, whereas the IC_{50} for K17F was 0.6 ± 0.2 nmol/l (**Fig. S1B**), as previously described [22].

To ensure the selectivity of action of LIT01-196 on the apelin-R and not on the V2-R, we assessed whether LIT01-196 modified cAMP production induced by V2-R stimulation. In HEK-293 T cells expressing the human V2-R, we observed that both LIT01-196 and K17F at a supramaximal concentration of 1 µmol/l did not modify cAMP production induced by 1 µmol/l AVP. Furthermore, K17F or LIT01-196 alone at 1 µmol/l did not modify basal cAMP production in these cells (**Fig. 2B**). We also verified that K17F and LIT01-196 were able to inhibit forskolin-induced cAMP production in a highly differentiated murine renal cortical collecting duct principal cell line (mpkCCD cells). We found in these cells that K17F (1 µmol/l) and LIT01-196 (1 µmol/l) significantly inhibit cAMP production induced by forskolin (1 µmol/l) by 33 % and 32 %, respectively (**Fig. 2C**). Finally, we checked whether K17F and LIT01-196 were able to inhibit dDAVP-induced cAMP production in mpkCCD cells. We observed that K17F (10 µmol/l) and LIT01-196 (10 µmol/l) inhibit dDAVP-induced cAMP production by 75% and 79%, respectively (**Fig. 2D**).

Effects of K17F and LIT01-196 on dDAVP-induced cAMP production in microdissected rat outer medullary collecting ducts

We previously showed that dDAVP, a specific and selective V2-R agonist, induced a maximal increase in cAMP production in rat outer medullary collecting ducts (OMCDs) at a concentration of 0.1 nmol/l, and the EC_{50} was 35 pmol/l [28]. We show here, in the same experimental conditions, that applying dDAVP (0.1 nmol/l) to microdissected rat OMCDs increased cAMP production (92.6 ± 3.6 vs. 19.3 ± 0.8 fmol cAMP/mm tubular length/10 min for dDAVP and baseline cAMP values, respectively, $P<0.001$, $n=6$). The co-application of dDAVP (0.1 nmol/l) with K17F or LIT01-196 in increasing concentrations (from 50 nmol/l to 50 µmol/l) progressively and significantly inhibited dDAVP-induced cAMP production by 45% and 41%, respectively, in the OMCDs (**Fig. 2E**).

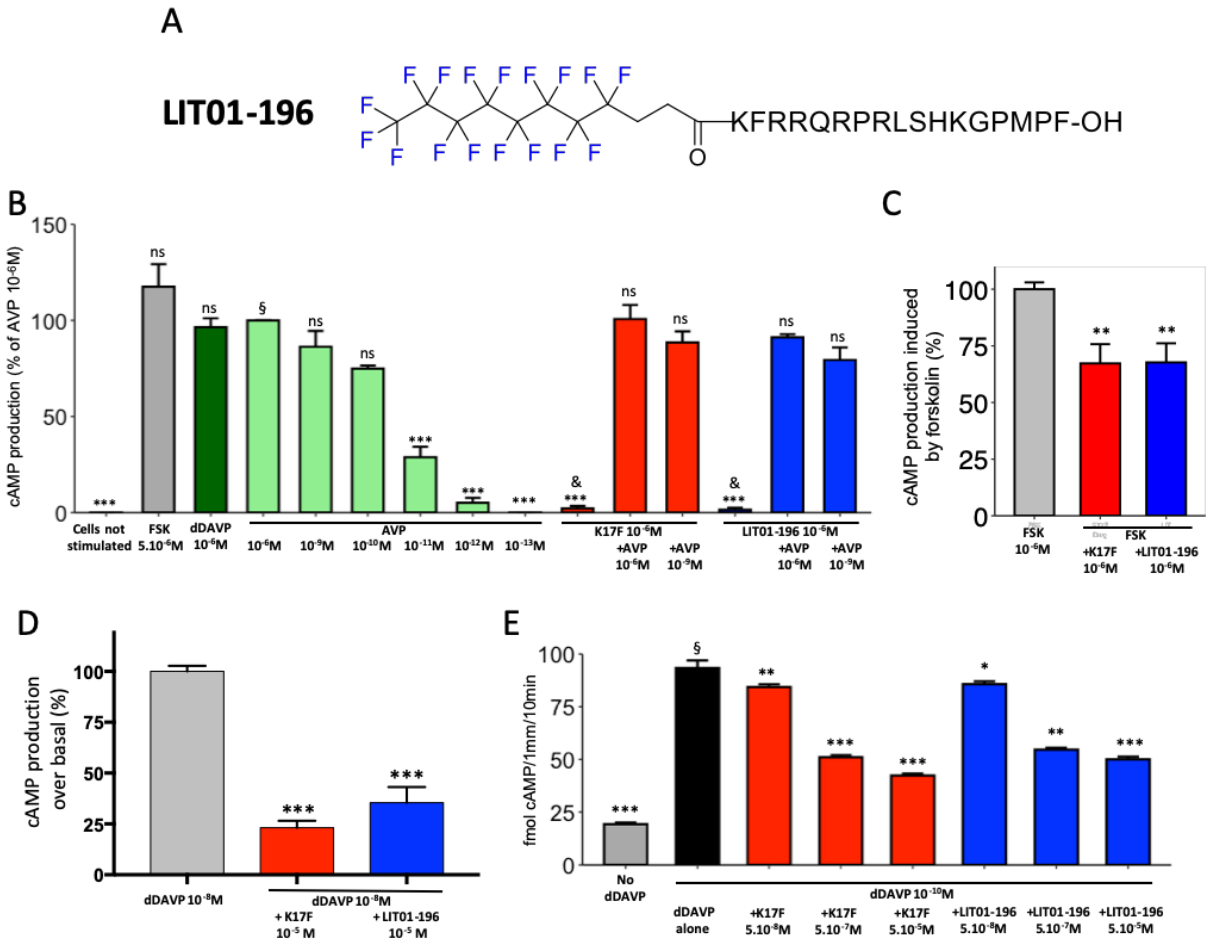

Fig. 2. *In vitro* and *ex vivo* effects of LIT01-196 on forskolin- or dDAVP-induced cAMP production. (A) Chemical structure of LIT01-196. **(B)** Effects of forskolin (FSK, 5 µmol/l), dDAVP (1 µmol/l), AVP (different concentrations), K17F (1 µmol/l) and LIT01-196 (1 µmol/l), and of the combination of either K17F (1 µmol/l) or LIT01-196 (1 µmol/l) with AVP (1 µmol/l and 1 nmol/l) on cAMP production in HEK-293 T cells expressing the human V2-R. Results are expressed as the percentage of increase from basal levels (cells not stimulated) induced by AVP (1 µmol/l). Four individual determinations were performed. Each point was compared to AVP (1 µmol/l); & denotes the absence of statistical difference with basal levels (cells not stimulated). **(C)** Effects of K17F (1 µmol/l) and LIT01-196 (1 µmol/l) on forskolin (1 µmol/l) - induced

cAMP production in mpkCCD cells for 30 min at 37°C. Each data represents the mean of four independent experiments performed in quadruplate and expressed as the mean ± S.E.M. ** $p<0.01$ when compared to forskolin alone. **(D)** Effect of K17F and LIT01-196 treatment on dDAVP-induced cAMP production. mpkCCD cells grown on permeable inserts were treated with depletion medium containing 10 nmol/l of dDAVP or in combination of dDAVP and 10 µmol/l K17F or LIT01-196B for 60 min at 37°C. Each data represent the mean of 3 independent experiments performed in quadruplicate and expressed as the mean ± S.E.M.. *** $p<0.001$ when compared to dDAVP alone **(E)** Effects of 0.1 nmol/l dDAVP on cAMP production in microdissected rat outer medullary collecting ducts in the presence or absence of different concentrations (50 nmol/l, 500 nmol/l and 50 µmol/l) of K17F or LIT01-196. Six individual determinations were performed. Each point was compared to dDAVP (10^{-6} mol/l). § denotes a statistical difference ($p<0.001$) with basal levels (No dDAVP).

Effects of K17F and LIT01-196 on dDAVP-induced phosphorylation of AQP-2 in mpkCCD cells

As expected from the literature[29,34], we observed an increase in the phosphorylation of AQP-2 at the apical membrane of the mpkCCD cells treated with 10 nmol/l of dDAVP for 1h. When mpkCCD cells were co-treated with K17F (10 µmol/l) or LIT01-196 (10 µmol/l) we observed a decrease in the phosphorylation of AQP-2 as shown by the decrease of the immunolabelling of the phosphoAQP-2 (**Fig. 3**).

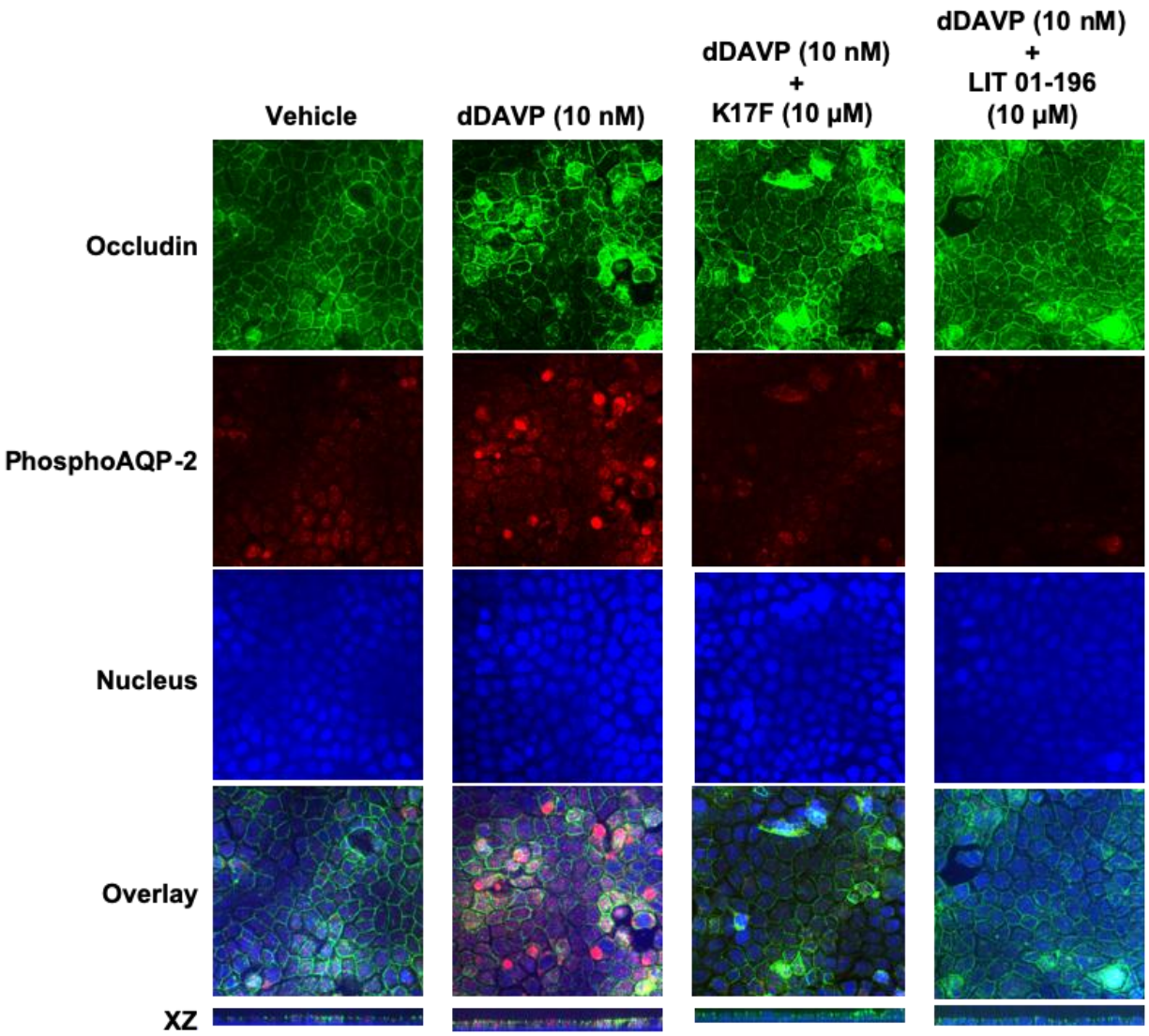

Figure 3. Effect of K17F and LIT01-196 treatment on dDAVP-induced phosphorylation of aquaporine 2. mpkCCD cells were grown on transwell filters for 5 days. After 24h of starvation cells were treated with vehicle or 10 nmol/l of dDAVP with or without 10 µmol/l of K17F or LIT01-196. Images are shown in XY and XZ plans and represent the immunofluorescence staining with an anti-occluding (green) and an anti-PhosphoAQP-2 (red) and the staining of the nuclei with DAPI (blue).

In vivo half-lives of K17F and LIT01-196

Plasma apelin levels were measured by RIA, with the K17F antiserum that we produced and characterized in a previous study [20]. The antibody directed against K17F recognized K17F,

pE13F and LIT01-196 with a similar affinity (IC_{50}: 0.11 ± 0.01 nmol/l for K17F, 0.26 ± 0.03 nmol/l for pE13F, 0.57 ± 0.05 nmol/l for LIT01-196, **Fig. 4A).** It does not recognize K16P[20] or Fluoro-K16P (IC_{50} > 1.0 µmol/l for Fluoro-K16P). We determined plasma apelin concentrations at baseline and at different times after the i.v. administration of K17F (250 nmol/kg, i.v.) or LIT01-196 (15 nmol/kg, i.v. or 900 nmol/kg, s.c.) to Sprague-Dawley rats and mice. Plasma apelin concentrations correspond to apelin levels at baseline or to apelin plus LIT01-196-immunoreactive (IR) material after LIT01-196 injection in alert control animals, thus enabling to estimate the *in vivo* half-life of LIT01-196. We estimated the *in vivo* half-life of K17F in the rat blood circulation at 50 seconds (**Fig 4B**), accounting for the very brief (2 minutes) decrease in blood pressure and increase in heart rate observed in rats following the i.v. injection of K17F [40]. In conscious mice, basal plasma apelin levels were 0.98 ± 0.09 pmol/ml. Five seconds after the i.v injection of K17F (250 nmol/kg), plasma apelin levels had risen to 49.2 ± 7.95 pmol/ml, 50 times basal levels. Plasma apelin concentration decreased rapidly after 60 seconds, reaching 2.8 times the basal level after 300 seconds (**Fig. S2A)**. The *in vivo* half-life of K17F in the mouse blood circulation has been estimated at 44 seconds, very similar to that obtained in rats (50 seconds) . Both i.v. and s.c. administrations of LIT01-196 to alert rats and mice led to a large increase in plasma apelin-IR levels. We estimated that the *in vivo* half-life of LIT01-196 in the blood circulation in alert rats was 28 minutes after i.v. administration (**Fig. 4C**) and 156 min after a s.c. administration (**Fig. 4D**). Using mass spectrometry, we evaluated the half-life of LIT01-196 after its injection by i.v. route at the dose of 300 nmol/kg in mice **(Fig. 4E)**, that was estimated at 25 min, close to that obtained in rats after i.v. administration (28 min) by using the RIA technique. To explain the higher plasma stability of LIT01-196 as compared to apelin, we explored the possibility that the fluorocarbon chain could bind to plasma proteins resulting in the

protection of the peptide from enzymatic degradation by steric hindrance. By the classical Diamon equilibrium dialysis chamber analysis[41] we showed that the bound fraction of LIT01-196 to plasma proteins was 69 ± 7% (value reached at equilibrium).

Plasma apelin levels 30 min after s.c. administration of LIT01-196 (900 nmol/kg, **Fig. 5F**) to Sprague Dawley rats were 1.3 ± 0.22 pmol/ml, 3.6 times higher than basal levels (0.36 ± 0.05 pmol/ml, p=0.008). Conversely, no change was observed in apelin-IR levels measured in the brain of rats treated with LIT01-196 (1.3 ± 0.14 pmol/brain) compared to basal values obtained in rats treated with saline (1.2 ± 0.15 pmol/brain, p=0.84, **Fig. 4G)**. The increase in plasma apelin-IR was also observed in mice 30 min after s.c. administration of LIT01-196 (900 nmol/kg, **Fig. S2B**). Plasma apelin-IR levels had risen to 12.4 ± 2.5 pmol/ml, 9.7 times basal levels (1.3 ± 0.073 pmol/ml, p=0.01). At the opposite, no change was observed in apelin-IR levels measured in the brain of mice treated with LIT01-196 (0.440 ± 0.073 pmol/brain) compared to basal values obtained in mice treated with saline (0.391 ± 0.045 pmol/brain, p=0.8, **Fig. S2C**).

Effects of K17F and LIT01-196 given by i.v. route on urine output in normonatremic rats

We evaluated the effects on urine output of an intravenous (i.v.) administration of K17F and LIT01-196 in control Sprague-Dawley rats. The i.v. injection of K17F (400 nmol/kg, 855 µg/kg) induced no significant change in 24-hour urine output or in urine osmolality in control rats. By contrast, the i.v. administration of LIT01-196 at a dose 27 times lower (15 nmol/kg, 51 µg/kg) induced a 93% increase in urine output (p<0.01) **(Fig. S2D)** and a 38% decrease in urine osmolality (p<0.01) relative to the values obtained for rats receiving saline i.v. (**Fig. S2E**). The i.v. administration of K17F or of LIT01-196 did not induce a significant change in water intake (**Fig S2F**).

Effects of LIT01-196 and tolvaptan given by s.c. route on metabolic parameters in normonatremic rats

We first determined in normonatremic rats the optimal dose of LIT01-196 to induce aqueous diuresis. Subcutaneous LIT01-196 from 300 to 900 nmol/kg induced a progressive increase in diuresis and a decrease in urine osmolality. The maximal effect was observed for doses comprised between 900 and 2400 nmol/kg. The effects of LIT01-196 and tolvaptan on urine output and osmolality were similar at an equimolar dose of 900 nmol/kg. However, increasing the dose of tolvaptan to 6700 nmol/kg was associated with an increased effect on urine output and urine osmolality, while increasing the dose of LIT01-196 to 2400 nmol/kg did not significantly increase its aquaretic effect ~~**of LIT01-196**~~ (**Fig. S3A and S3B).** We thus used the dose of 900 nmol/kg to study the effects LIT01-196, and compared them to both the equimolar dose of tolvaptan and to a higher dose.

In addition, we compared the kinetics of the effects of LIT01-196 and tolvaptan on metabolic parameters in alert normonatremic Sprague-Dawley rats. Relative to saline (*n*=19), LIT01-196 (900 nmol/kg, *n*=23) and tolvaptan (900 nmol/kg, *n*=12) significantly increased 24 h-urine output by 108% and 110%, respectively. Urine osmolality decreased similarly in the two groups, by 51% in animals receiving LIT01-196 and 40% in animals receiving tolvaptan. Although the aquaretic effect of tolvaptan was significant at 3, 6 and 24 hours after administration, the aquaretic effect of LIT01-196 was only significant 24 hours after administration, showing an effect occurring later with this compound **(Fig. 4 H-I**). Increasing the dose of LIT01-196 to 2400 nmol/kg did not result in an earlier effect on aqueous diuresis **(Fig. S3 C-D).** The increase in urine output was associated with a significant increase in water intake **(Fig. 4J)** in the tolvaptan group (+37%) and a slight increase in the LIT01-196 group (+11%). Food (normal chow) intake

(Fig. 4K) was similar in the saline and the tolvaptan groups but slightly and non-significantly lower in animals receiving LIT01-196 (20% decrease). Water intake to food intake ratio was significantly increased by 50% in the LIT01-196 group and non-significantly increased by 24% in the tolvaptan group **(Fig. 4L)**. A slight weight loss (-1.8%) (**Fig. 4M**) was observed in the LIT01-196 group.

Tolvaptan at a higher dose (6700 nmol/kg, n=13) induced a larger aquaretic effect than LIT01-196 at both 900 and 2400 nmol/kg (**Fig S4 A-B**), that occurred more rapidly than with LIT01-196 (**Fig S3 C-D**). LIT01-196 (900 nmol/kg) significantly increased free water excretion fraction by 86%, while tolvaptan (6700 nmol/kg) induced a similar but non-significant increase **(Fig. S4C).** Sodium excretion fraction **(Fig. S4D)** was not significantly modified by the administration of LIT01-196 (900 nmol/kg) or tolvaptan (6700 nmol/kg).

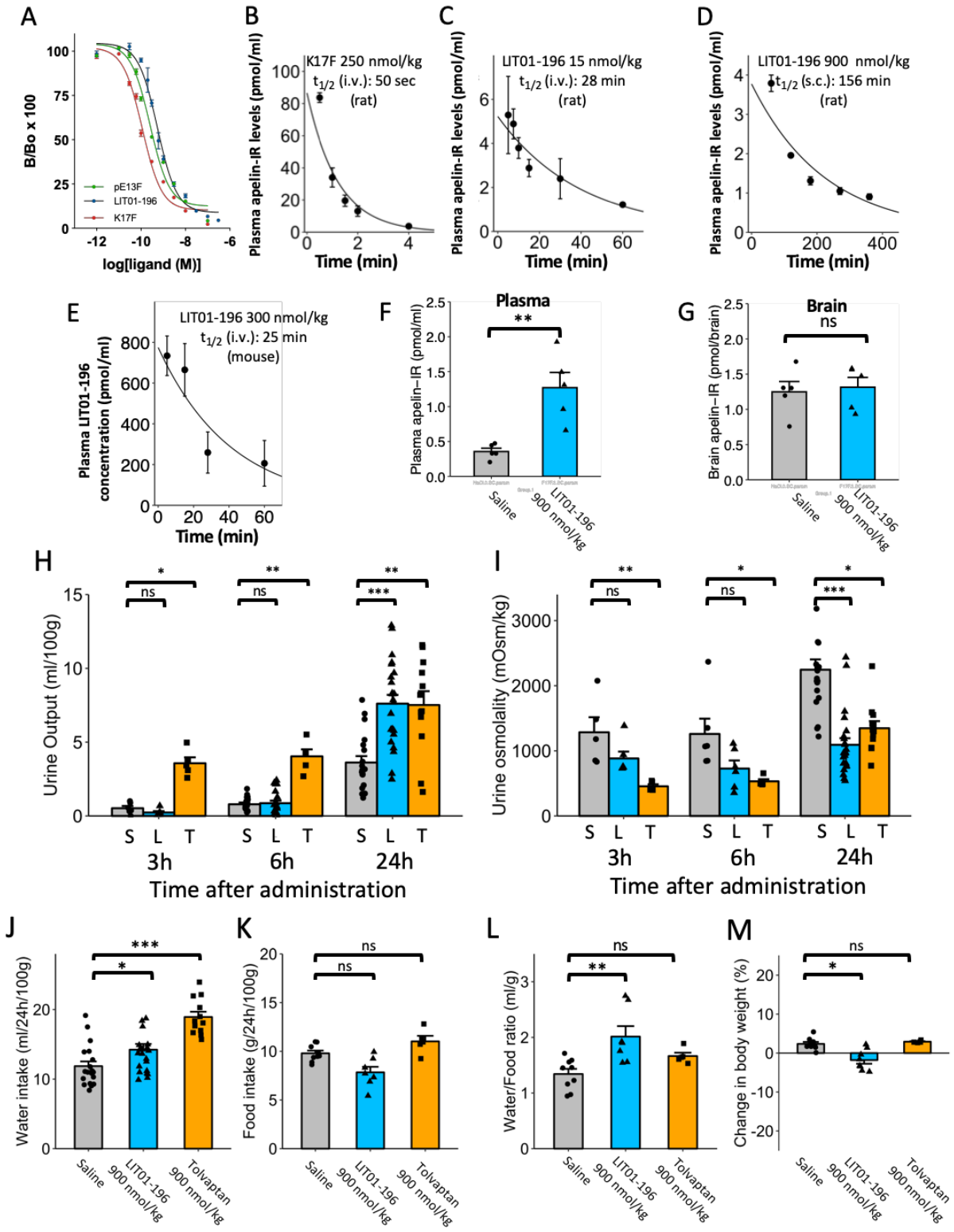

Fig 4. ***In vivo*** **half-life of K17F and LIT01-196 and effects of s.c. saline, tolvaptan, LIT01-196 on water metabolism, food intake, body weight, plasma electrolytes in control rats. (A)**

Inhibition of [^{125}I]-pE13F binding to anti-K17F serum (1/18000 final dilution) by unlabeled K17F, pE13F or LIT01-196. Data are expressed as a percentage of the maximal binding of [^{125}I]-pE13F in the absence of non-radiolabeled ligand and represent three independent experiments performed in triplicate. **(B)** *In vivo* half-life of K17F following i.v. administration in rats. K17F (250 nmol/kg i.v.) was injected in alert rats. Animals (n=3-6 per time point) were killed at various times following injection, trunk blood was collected and plasma apelin-immunoreactive levels were determined in a radioimmunoassay. **(C)** *In vivo* half-life of LIT01-196 following i.v. administration in rats. LIT01-196 (15 nmol/kg i.v.) was administered to alert rats. Animals (n=3-6 per time point) were killed at various times following injection, trunk blood was collected and plasma apelin-immunoreactive levels were determined in a radioimmunoassay. **(D)** *In vivo* half-life of LIT01-196 following s.c. administration (900 nmol/kg) in rats. Animals (n=3-6 per time point) were killed at various times following injection, trunk blood was collected and plasma apelin-immunoreactive levels were determined in a radioimmunoassay. **(E)** *In vivo* half-life of LIT01-196 following i.v. administration in mice (3 animals per time point). LIT01-196 (300 nmol/kg i.v.) was administered to alert mice and plasma LIT01-196 concentration was determined by mass spectrometry analysis. **(F)** Plasma and **(G)** brain apelin-immunoreactive levels in rats (n=5) 30 minutes after subcutaneous administration of saline or of LIT01-196 (900 nmol/kg). **(H-M)** *In vivo* effects of s.c. saline, tolvaptan, LIT01-196. Evaluation of the effect of saline (1 ml/kg, n=19); LIT01-196 (900 nmol/kg, n=23) and tolvaptan (900 nmol/kg, n=12) in alert male Sprague-Dawley (SD) rats given normal chow on **(H)** Urine output and **(I)** urine osmolality measured 3, 6 and 24 hours after saline (S), LIT01-196 (L) and tolvaptan (T). Metabolic parameters were measured 24 hours after the s.c. administration of saline, LIT01-196 or tolvaptan (**J**, water intake; **K**, food intake; **L**, water to food intake ratio; **M**, body weight change). Multiple comparisons performed by Kruskal-Wallis followed by post-hoc Dunn's tests with Holm's adjustment. Ns: $p>0.05$, *$P<0.05$, **$P<0.01$, ***$P<0.001$.

Effects of LIT01-196 and tolvaptan on plasma AVP and apelin levels in control rats

Plasma AVP and apelin (apelin-immunoreactive (IR) material) levels were measured three hours after the s.c. administration of saline (n=9), tolvaptan (6700 nmol/kg s.c., n=6) and LIT01-196 (900 nmol/kg s.c., n=8) into alert rats (**Fig. S4 E-G**). Rats receiving tolvaptan had significantly

higher plasma AVP levels (134% higher; $P<0.001$) than control animals receiving saline, and no change in plasma AVP levels was observed in rats receiving LIT01-196.

Plasma apelin-IR levels in control rats (receiving saline) and in rats receiving tolvaptan were similar. Plasma apelin-IR levels in rats receiving LIT01-196 were significantly higher (140%) than those in control rats ($p<0.001$). Plasma apelin/AVP ratio was not significantly different in rats receiving tolvaptan or saline, but was higher in rats receiving LIT01-196 (91% higher than in control rats; $p=0.003$).

Effects of LIT01-196 on blood pressure, cardiac contractility, kidney function and blood glucose

Following s.c. injection of LIT01-196 (900 nmol/kg) in alert Sprague-Dawley rats, mean arterial blood pressure (MABP) decreased slightly 3 hours after administration, and this change did not reach statistical significance (baseline MABP, 106±2 mmHg, MABP three hours after LIT01-196 administration, 94±2 mmHg, p=0.063, n=5). MABP measured 24 hours after administration of LIT01-196 did not significantly differ from baseline (p=0.88) **(Fig. S5A).** We also evaluated the effects of s.c. LIT01-196 administration on left ventricular ejection fraction (LVEF) estimated by echocardiography in mice (n=5) and did not observe any significant effect at the slightly higher dose of 1200 nmol/kg (LVEF 3 hours after administration, 57.1 ± 0.7 % vs 52.6 ± 3.0 % before administration, p=0.31) **(Fig. S5B)**. Following the s.c. administration of LIT01-196 at the dose of 900 nmol/kg for 4 consecutive days, we performed histological analysis of the kidneys that did not reveal any abnormality (**Fig. S5 C-F**). Blood creatinine, urea nitrogen, sodium and potassium levels (**Fig. S5G-J**) were not changed by LIT01-196 treatment. Repeated administration of LIT01-196 (900 nmol/kg, s.c.) to normonatremic Sprague Dawley rats was not associated with a change in plasma or urine glucose levels (**Fig. S5K and S5L**).

Establishment of a rodent model of AVP-induced hyponatremia

We established a rodent model of AVP-induced hyponatremia by administering AVP subcutaneously and continuously via an osmotic minipump in male Sprague-Dawley rats placed in metabolic cages and fed a liquid diet. The effects of different doses of AVP on urine output, urine osmolality and plasma sodium, water and food intake were evaluated. For a dose of 30 or 50 ng AVP/hour, urine output decreased during the four days following insertion of the osmotic minipump (mean decrease of 61% in rats receiving AVP at a dose of 30 ng/h relative to rats receiving saline), urine osmolality increased by 455% and plasma sodium concentration decreased by 26% ($p<0.001$ for urine output, urine osmolality and plasma sodium). Animals treated with AVP at a dose of 30 ng/h or higher also decreased their food and water intake ($p<0.001$) (**Fig. S6**). Little or no effect was observed with a lower dose of AVP (20 ng AVP/h). A moderate decrease in body weight was observed during the experiment in both hyponatremic and normonatremic animals, even in the absence of AVP administration, but weight loss was significantly greater in animals receiving 30 ng/h AVP or more (**Fig. S6D**). The experiment was stopped after five days because some of the animals had lost more than 20% of their body weight, the acceptable limit established with the ethics committee. The minimum effective dose of AVP (30 ng/h) was therefore used to study the effects of aquaretic agents on AVP-induced hyponatremia.

Determination of the optimal dose of LIT01-196 in hyponatremic rats

We then determined that the administration of both LIT01-196 and tolvaptan, at the dose of 900 nmol/kg, induced a similar increase in diuresis in the 24 hours following s.c. administration in rats receiving 30 ng/h AVP and a liquid diet (increase of 11.7 ± 2.3 and 9.5 ± 2.9 ml/24h/100g, respectively). In contrast, urine output did not change 24 hours after administration of saline. The

use of a lower dose of LIT01-196 (180 nmol/kg s.c.) was associated with a smaller increase of urine output (increase of 1.5 ± 2.0 ml/24h/100g), while increasing the dose of LIT01-196 to 2400 nmol/kg did not increase the effect of the compound on urine output (increase of 9.2 ± 4.1 ml/24h/100g). In contrast, increasing the dose of tolvaptan to 6700 nmol/kg led to an even greater increase in urine output (increase of 27 ± 9.0 ml/24h/100g). Given these results, we used the identical dose of 900 nmol/kg to compare the metabolic effects of LIT01-196 and tolvaptan in a model of AVP-induced hyponatremia.

Evaluation of the effects of LIT01-196 and tolvaptan in a model of AVP-induced hyponatremia

As described above, a minipump administering 30 ng AVP/h s.c. was implanted two days before the administration of an aquaretic treatment (tolvaptan or LIT01-196) or saline, and all animals received a semi-liquid diet (50% water, 50% gel-diet, as described in Methods). Water consumption included water mixed with the food as well as water consumed from the bottle. (experimental protocol, **Fig. 5A**). Four experimental groups were studied: the control group (receiving no AVP, n=7), the AVP + saline group (continuous s.c. infusion of 30 ng AVP/h + saline 1 ml/kg s.c. on days 0 and 1, n=13), the AVP + tolvaptan group (30 ng AVP/h s.c. + tolvaptan 900 nmol/kg s.c. on days 0 and 1, n=12) and the AVP + LIT01-196 group (30 ng AVP/h s.c. + LIT01-196 900 nmol/kg s.c. on days 0 and 1, n=9). On day 0, before treatment administration, plasma sodium levels were low and similar in all animals receiving AVP (103 ± 1, 103 ± 1 and 101 ± 3 mmol/l, p=0.6, for the AVP + saline, AVP + tolvaptan and AVP + LIT01-196 groups, respectively). Animals receiving AVP + saline had significantly lower urine output than controls (49% lower on average between day 1 and day 2, P=0.002), higher urine osmolality (355% higher, P<0.001), lower water intake (59% lower, P<0.001) and lower plasma sodium

levels (27% lower, $P<0.001$). These parameters remained stable from day 0 to day 2 (**Fig. 5 B-E**).

We then evaluated the effects of LIT01-196 in hyponatremic rats. The model was set up as described above, and LIT01-196 (900 nmol/kg s.c.) was administered on days 0 and 1. Relative to AVP-treated animals receiving saline, the LIT01-196-treated animals had significantly higher urine output (185% higher, on average, from day 1 to day 2, relative to the AVP + saline group, $P<0.001$), and lower urine osmolality (58% lower, $P<0.001$). An increase in plasma sodium concentration was observed on day 1, 24 hours after the first administration of LIT01-196, relative to animals receiving saline (109 ± 5 versus 100 ± 2 mmol/l), and on day 2 (110 ± 5 versus 100 ± 2 mmol/l), and plasma sodium concentration after LIT01-196 administration were significantly higher than in the AVP + saline group ($P=0.042$). Following treatment with LIT01-196, AVP-treated animals had 177% higher levels of water consumption (including water in diet), on average, from day 1 to day 2 ($P<0.001$, versus the AVP + saline group) (**Fig. 5B-E**). LIT01-196 treatment was associated with a significant increase in food consumption, and thereby a significant increase in sodium intake. Body weight change from baseline was similar in AVP-treated animals receiving LIT01-196 and saline (**Fig. S7**). Subcutaneous administration of tolvaptan at the same dose (900 nmol/kg) on days 0 and 1 was associated with a similar effect on urine output, urine osmolality, plasma sodium and water intake (**Fig. 5B-E**).

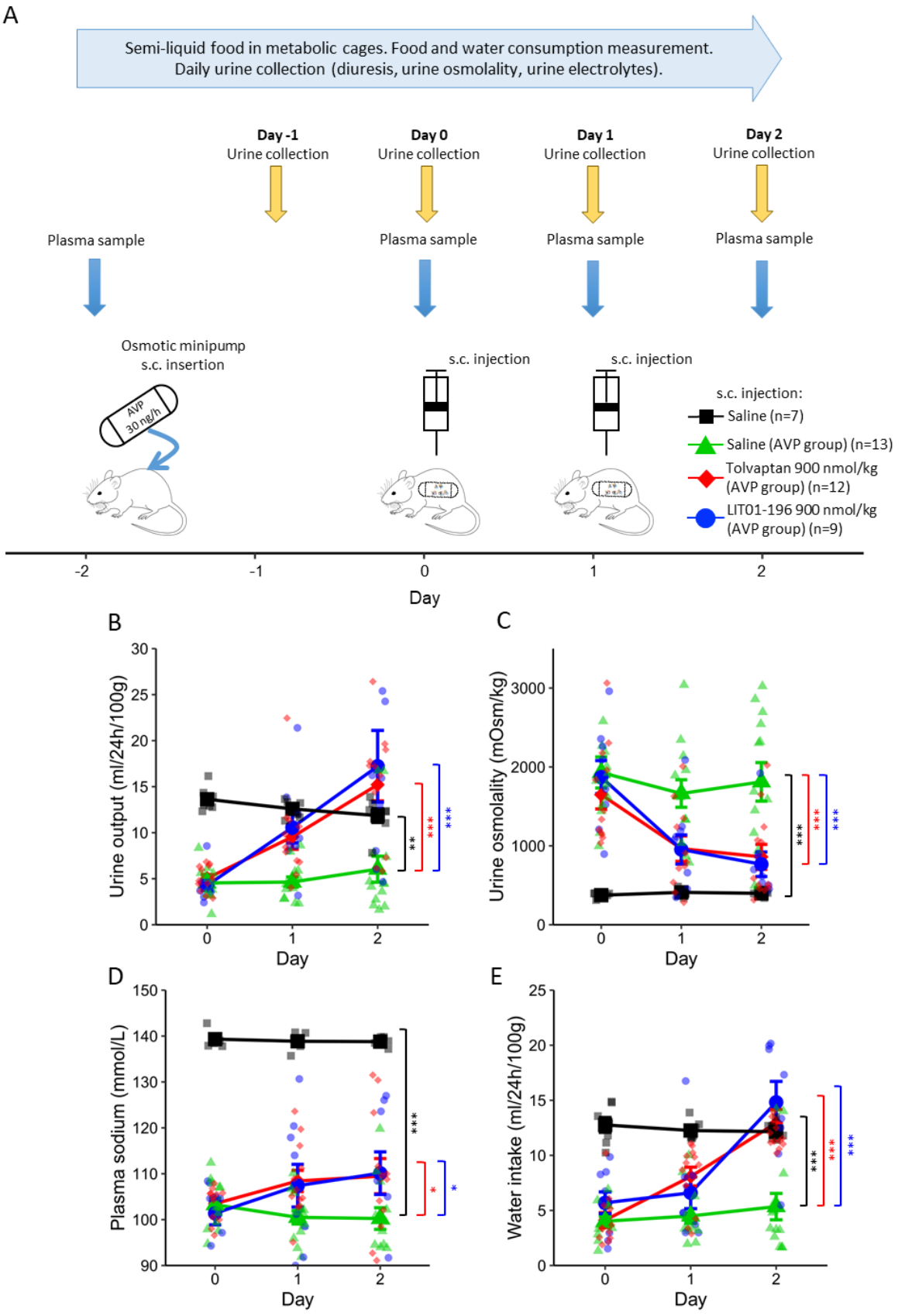
A
Semi-liquid food in metabolic cages. Food and water consumption measurement.
Daily urine collection (diuresis, urine osmolality, urine electrolytes).
Day -1
Urine collection
Day 0
Urine collection
Day 1
Urine collection
Day 2
Urine collection
Plasma sample
Plasma sample
Plasma sample
Plasma sample
Osmotic minipump
s.c. insertion
AVP
30 ng/h
s.c. injection
s.c. injection
s.c. injection:
Saline (n=7)
Saline (AVP group) (n=13)
Tolvaptan 900 nmol/kg
(AVP group) (n=12)
LIT01-196 900 nmol/kg
(AVP group) (n=9)
-2
-1
0
1
2
Day
B
Urine output (ml/24h/100g)
Day
C
Urine osmolality (mOsm/kg)
Day
D
Plasma sodium (mmol/L)
Day
E
Water intake (ml/24h/100g)
Day
Saline
AVP+saline
AVP+tolvaptan 900 nmol/kg s.c.
AVP+LIT01-196 900 nmol/kg s.c.

Fig. 5. Effects of saline, tolvaptan and LIT01-196 on water metabolism and plasma electrolytes in hyponatremic rats. (A) Experimental protocol for generating hyponatremia. On day -2, a plasma sample was collected from the tail vein of each animal (male SD rats). Except for the control group, which received no AVP, a subcutaneous osmotic minipump delivering AVP at a rate of 30 ng/h was then implanted into each animal. All the animals were given semi-liquid food. On day 0, a plasma sample was collected and each animal treated with AVP received a s.c. injection of saline (green curve, 1 ml/kg, *n*=13), tolvaptan (red curve, 900 nmol/kg, *n*=12) or LIT01-196 (blue curve, 900 nmol/kg, *n*=9). Animals not treated with AVP received a s.c. injection of saline (black curve, *n*=7). On day 1, plasma samples were obtained and each animal received another administration of the same treatment. On day 2, a final plasma sample was collected and the animals were killed. Urine output was measured and analyzed every day from day -1 to day 2, and water and food intake were also measured daily. Change in 24-hour urine output **(B)**, urine osmolality **(C)**, plasma sodium concentration **(D)** and water intake (including water in the bottle and in the food) **(E)** in animals receiving continuous s.c. AVP at a rate of 30 ng/h from day -2 to 2, and a s.c. injection of saline (green curve, *n*=13), tolvaptan (red curve, 900 nmol/kg, *n*=12) or LIT01-196 (blue curve, 900 nmol/kg, *n*=9) on days 0 and 1. The black curve represents animals receiving no AVP (*n*=7); all animals received a semi-liquid diet. Each group was compared with the AVP + saline group with a linear mixed-effects model, to take repeated measurements over time into account; ns: $P>0.05$, *$P<0.05$, **$P<0.01$, ***$P<0.001$.

Plasma AVP and apelin levels following the administration of LIT01-196 or tolvaptan in hyponatremic rats

Plasma AVP and apelin-IR levels were measured after the continuous administration of AVP (30 ng/h) for 48 hours in male Sprague-Dawley rats receiving a semi-liquid diet, 3 hours after the administration of saline (AVP + saline), LIT01-196 (900 nmol/kg, AVP + LIT01-196) or tolvaptan (6700 nmol/kg, AVP + tolvaptan) and in rats receiving the same diet but no AVP (**Fig. 6**). The continuous administration of AVP (30 ng/h) for 48 hours significantly increased plasma AVP levels by 120% in animals receiving AVP + saline (**Fig. 6A**). No significant difference in AVP levels was observed between AVP-treated rats receiving saline or LIT01-196. Plasma

apelin levels were similar in animals receiving no AVP and in those receiving AVP + saline, but plasma apelin immunoreactive (IR) material levels were 372% higher in rats receiving AVP + LIT01-196 than in rats receiving AVP + saline, because the antibody against K17F recognizes K17F and LIT01-196 with similar affinity (**Fig. 6B**). In hyponatremic rats, LIT01-196 treatment increased plasma apelin-IR/AVP ratio by 518% relative to rats receiving saline **(Fig. 6C)**. Plasma AVP and apelin levels in rats receiving AVP + tolvaptan were similar to those in animals receiving AVP + saline.

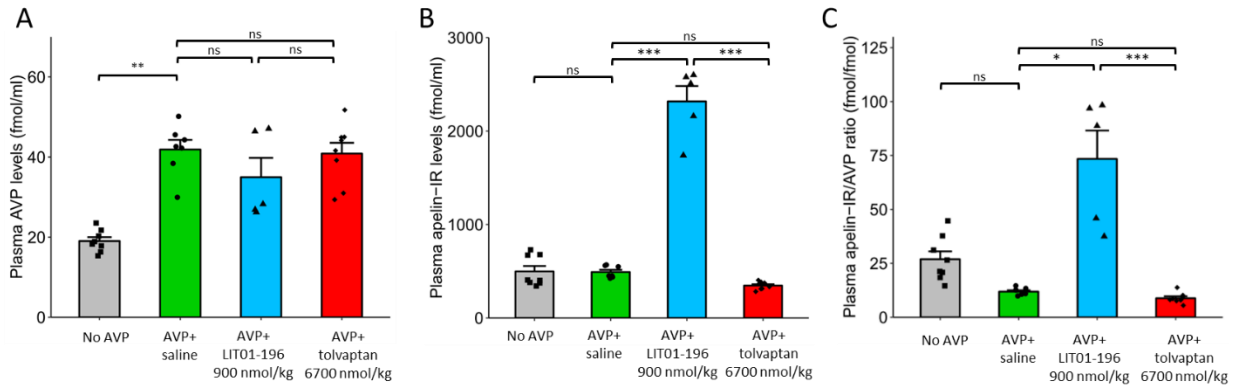

Fig. 6. Plasma AVP and apelin levels in hyponatremic rats receiving saline, LIT01-196 and tolvaptan, relative to normonatremic rats. Measurements of plasma AVP levels **(A)**, plasma apelin-IR levels **(B)** and plasma apelin-IR/AVP ratios **(C)** in alert male Sragues-Dawley rats receiving a semi-liquid diet and no AVP (grey bars, *n*=8), a 48-hour s.c. infusion of AVP at a rate of 30 ng/h together with a s.c. injection of saline (green bars, 1 ml/kg, *n*=7), LIT01-196 (blue bars, 900 nmol/kg, *n*=5) or tolvaptan (red bars, 6700 nmol/kg, n=8) three hours before blood collection. Multiple comparisons performed by Kruskal-Wallis followed by post-hoc Dunn's tests with Holm's adjustment. Ns: $p>0.05$, *$P<0.05$, **$P<0.01$, ***$P<0.001$.

Discussion

We demonstrate in this study that the s.c. administration of LIT01-196, a metabolically stable K17F analog, in a rat experimental model of AVP-induced hyponatremia blocks the AVP-induced decrease in urine output and increase in urinary osmolality, leading to a progressive correction of hyponatremia. These results provide evidence for a major role of apelin, together with AVP, in the regulation of body fluid homeostasis and suggest that the use of apelin-R agonists may represent a new approach for the treatment of hyponatremia.

LIT01-196 was previously shown to display, like K17F, full agonist activity for the apelin-R stably expressed in CHO cells, for inhibiting forskolin-induced cAMP production, inducing ERK1/2 phosphorylation, apelinR internalization and β-arrestin recruitment[22]. In addition, LIT01-196 had a plasma half-life superior to 24 h versus 4.6 min for K17F[22]. In the present study, we show that LIT01-196, similarly to K17F, dose-dependently inhibits dDAVP-induced cAMP production in CHO cells stably expressing both the Apelin-R and the V2-R. In contrast, LIT01-196, even at a supramaximal concentration of 1µmol/l, does not inhibit AVP-induced cAMP production in HEK-293T cells, that overexpress the V2-R but not the ApelinR. This indicates that LIT01-196 does not inhibit dDAVP or AVP-induced cAMP production by binding to the V2-R and acting as a V2-R antagonist. Hence, LIT01-196 by binding to the Apelin-R, activates Gi-protein-coupling, counteracting the increase in cAMP production induced by dDAVP or AVP via Gs-protein coupling of the V2-R. Additional evidence that the inhibitory effect of LIT01-196 on dDAVP-induced cAMP production occurs via a non-V2 mediated mechanism is provided by the fact that LIT01-196 as K17F inhibits forskolin-induced cAMP production in mpkCCD cells, a collecting duct principal cell line expressing both the V2R and the apelin-R [29,34]. We also show that LIT01-196, similarly to K17F [28], inhibits the increase in

603 cAMP production induced by dDAVP in mpkCCD cells and also in freshly microdissected rat
604 OMCD, a more physiological preparation. To investigate if the inhibition by LIT01-196 of the
605 cAMP production induced by dDAVP results in a decrease in AQP-2 translocation to the apical
606 membrane, we show in mpkCCD cells that LIT01-196 greatly reduces dDAVP-induced apical
607 cell surface expression of phosphorylated AQP-2. These data are in agreement with previous
608 studies showing that i.v. administration of K17F into lactating rats inhibited the AVP-induced
609 AQP-2 insertion into the apical membrane of the CD and increased aqueous diuresis by
610 decreasing AVP-induced cAMP production in the CD [28]. These data suggested that systemic
611 LIT01-196 administration in rats could induce an increase in aqueous diuresis. Before assessing
612 the *in vivo* metabolic effects of LIT01-196, we first investigated the *in vivo* half-life of LIT01-
613 196 in the blood circulation after i.v. administration in alert control mice and rats, by using two
614 methods, mass spectrometry analysis and radioimmunoassay. Both yielded similar results, 25
615 and 28 min respectively for LIT01-196 versus only 44 and 50 seconds for K17F after i.v.
616 administration in mice and rats, respectively. We then showed in alert control rats that LIT01-
617 196 had an *in vivo* half-life in the bloodstream of 156 min after s.c. administration. The increase
618 of the *in vivo* half-life of LIT01-196 in the blood circulation is probably due to the binding of
619 LIT01-196 to plasma proteins leading to the protection from enzymatic degradation and the
620 reduction of renal clearance, as LIT01-196 has a 69% binding to plasma proteins. This led to
621 evaluate the effects of LIT01-196 on water metabolism.
622 The s.c. administration of LIT01-196 (900 nmol/kg) in control rats increases urine output,
623 decreases urine osmolality, modestly increases water intake, water intake / food intake ratio,
624 increases free water clearance while fractional sodium excretion is unchanged, demonstrating an
625 aquaretic effect. These data are similar to those obtained with tolvaptan, used as a positive

626 control, and administered at an equimolar dose, except for the increase water intake which is
627 higher with tolvaptan (+ 37%) than with LIT01-196 (+ 11 %). The slight increase in water intake
628 induced by LIT01-196 could be related to the fact that i.c.v. administration of apelin-13 in water-
629 deprived rats reduces water intake [24], although it increases water intake in normally hydrated
630 mice [42]. Moreover, in patients with primary polydipsia, plasma apelin levels are lower than in
631 healthy volunteers [43]. Altogether, these results suggest that activation of the apelin receptor may
632 limit water intake associated with aquaresis, without abnormally increasing plasma osmolality.

633 As we previously showed that i.c.v. administration of K17F, by reducing the release of AVP
634 from the posterior pituitary into the bloodstream, increased diuresis in lactating rats [20], it was
635 important to determine whether LIT01-196 given by s.c. route acted through central and/or renal
636 action. Especially, we wanted to determine if LIT01-196 could cross the blood-brain barrier
637 (BBB) after systemic administration. Neuronal apelinergic fibers have been visualized in the
638 lamina terminalis of rats, along the anteroventral third ventricle region, including the subfornical
639 organ (SFO), the organum vasculosum and the median preoptic nucleus [25] . These structures are
640 all interconnected and project both excitatory and inhibitory signals to the SON and PVN [44] to
641 regulate the activity of AVP/apelin magnocellular neurons which also express apelin-R [20,24] . We
642 show here in rats and in mice that 30 min after s.c. injection of LIT01-196 (900 nmol/kg), the
643 compound is abundant in the blood circulation but absent in the brain, showing that LIT01-196
644 does not cross the blood-brain barrier (BBB) and does not enter the brain. Furthermore, knowing
645 that among the circumventricular organs, only the SFO expresses apelin-R mRNA [45] and that the
646 administration of LIT01-196 by s.c. route at the dose of 900 nmol/kg does not modify AVP
647 release in the blood circulation, our results strongly suggest that LIT01-196 given by s.c. route at
648 this dose does not act on the SFO to regulate magnocellular vasopressinergic neuron activity and

systemic AVP release. Therefore, the observed effects of LIT01-196 administered s.c. on water metabolism result from the action of the compound at the kidney level.

As the s.c. administration of LIT01-196 increased aqueous diuresis, we investigated whether LIT01-196 could be used to reverse the antidiuretic effect of AVP *in vivo*. We found that a continuous s.c. infusion of AVP (30 ng/h) for four days together with a semi-liquid diet, led to a decrease in urine output and an increase in urine osmolality. We established that, at this dose, plasma AVP levels were 120% higher than those in rats receiving saline, and that plasma sodium levels were decreased and stable at about 100 mmol/l for two to four days after the initiation of AVP infusion. LIT01-196 administered in this rat hyponatremic model at the dose of 900 nmol/kg, for two days, via the s.c. route, inhibited the effects of AVP on urine output and urine osmolality highly efficiently, and induced a progressive correction of plasma sodium levels. Considering *ex vivo* and *in vivo* data, this suggests that LIT01-196 by acting on apelin-R present in the CD, inhibits the AVP-induced cAMP production, thereby inhibiting the insertion of AQP-2 at the apical membrane of the CD, resulting in the inhibition of water reabsorption by the kidney and an increase in aqueous diuresis (**Fig. 7**).

As expected from previous studies [7], tolvaptan also inhibited the antidiuretic effects of AVP. However, while tolvaptan and LIT01-196 at the same dose of 900 nmol/kg resulted similar aquaretic effects in both control and hyponatremic rats, increasing the dose of tolvaptan resulted in an even larger increase in urine output, while increasing the dose of LIT01-196 did not. Activating the apelin-R and thus modifying the apelin/AVP balance in the collecting duct, rather than blocking the effects of AVP, may therefore less often result in severe polyuria and be better tolerated than V2-R antagonists.

The apelin-R is widely expressed, as opposed to the V2-R, which could result in unwanted effects following LIT01-196 administration. Apelin has been reported in rodents to induce a transient decrease in blood pressure [46], to increase cardiac contractility [47] and to improve glucose tolerance [48]. However, LIT01-196 (900 nmol/kg) given by s.c. route in Sprague Dawley rats did not significantly modify mean arterial blood pressure, blood glucose levels and kidney function. LIT01-196 (1200 nmol/kg s.c.) did not modify left ventricular ejection fraction in mice. Repeated administrations of LIT01-196 were not associated with renal failure or histological alterations of the kidney, and plasma sodium, potassium and glucose levels were not affected by LIT01-196 administration in control rats. The various physiological effects associated with the activation of the apelin-R result from the activation of different signaling pathways. Hence, the development of biased apelin-R agonists that specifically target the protein Gi signaling pathway may improve their specificity of action regarding water metabolism.

In conclusion, LIT01-196 is a potent metabolically stable K17F analog that acts as an aquaretic agent. Our model mimics a clinical situation in which the osmotic regulation of circulating AVP levels is impaired, causing SIAD. In this context, LIT01-196 can inhibit the antidiuretic effect of AVP, by increasing urine output, decreasing urine osmolality, enhancing water intake moderately and progressively correcting hyponatremia. Furthermore, our study constitutes a proof of concept that through the activation of apelin-R, metabolically stable apelin analogs, represent promising candidates for the treatment of SIAD. Whether apelin-R agonists could also be beneficial in pathological situations where AVP secretion is in excess and plasma apelin levels are decreased [49], such as ADPKD, remain to be determined.

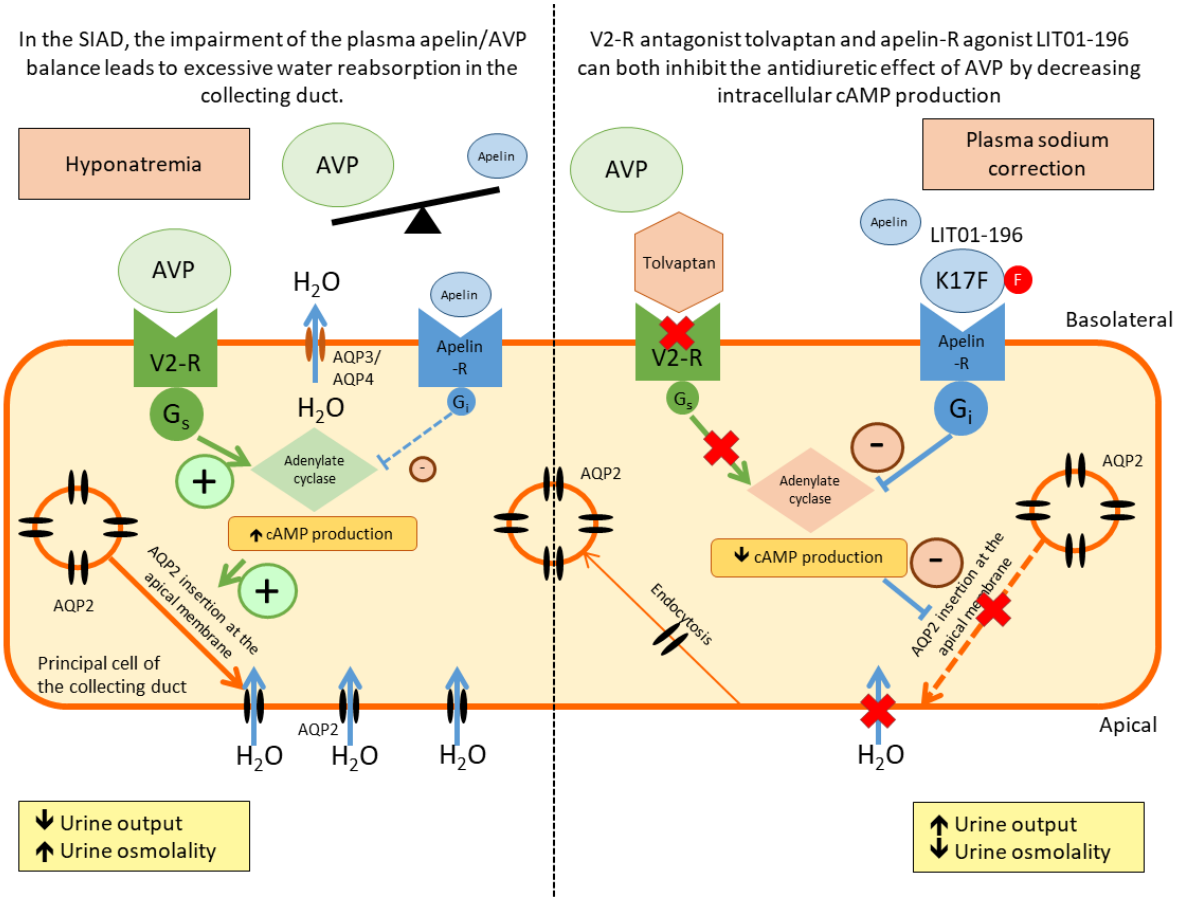

692

693 **Fig. 7. Proposed model of the effects of LIT01-196 on the principal cell of the collecting**

694 **duct in SIAD.**

695

696

697 **Acknowledgements**

698 The authors would like to thank Dr Solène Boitard, Gwladys Haslé and Paul Del Rincon from
699 the Laboratory of Central Neuropeptides in the Regulation of Body Fluid Homeostasis and
700 Cardiovascular Functions for animals and cell biology experiments, and Pr Nicolas Pallet, from
701 the Clinical Chemistry Department, Hôpital Européen Gorges Pompidou, APHP, Paris, France,
702 for biochemistry determinations. We are grateful to Nicolas Humbert (Laboratory of

Biophotonics and Pharmacology, Illkirch, France) for peptide synthesis, Patrick Gizzi and François Daubeuf for PK experiments (Plate-forme de Chimie Biologique Intégrative de Strasbourg, TechMedILL, UMS 3286 CNRS/Université de Strasbourg, Illkich). We acknowledge the Orion imaging facility, CIRB, for their support with the spinning-disk imaging and image analysis.

Funding

This work was supported by the *Institut National de la Santé et de la Recherche Médicale* (INSERM) including financial support for Proof of Concept, CoPoc Apelinatremia 2015-2017 by INSERM Transfert, the *Centre National de la Recherche Scientifique*, the *Université de Strasbourg*, the *LabEx MEDALIS*, the *Collège de France*, the *Agence Nationale de la Recherche* "Vie, santé et bien-être 2016" (ANR-16-CE18-0030, FluoroPEP), the *Fédération Française de Cardiologie* and the FRC (Frontier Research in Chemistry). AF was supported by a fellowship from INSERM (Poste d'Accueil pour Hospitaliers). PEGS was supported by a fellowship from the Fondation pour la Recherche Médicale. LE and SMR were supported by a fellowship from the *Ministère de l'Education Nationale, de l'Enseignement Supérieur et de la Recherche* and *the Agence Nationale pour la Recherche*, respectively.

Author contributions: AF designed the studies, conducted experiments, acquired and analyzed data, and wrote the manuscript; PEGS designed the studies, conducted experiments, analyzed data and wrote the manuscript; MK, RAP and NdM conducted experiments and analized the data; LE, SMR and DB performed the chemical synthesis of LIT01-196, conducted experiments and wrote parts of the manuscript. CLC supervised the work, designed the studies, analyzed the data, wrote the manuscript and ensured the funding.

Competing interests: None.

726

References

1. Ellison, D. H. & Berl, T. Clinical practice. The syndrome of inappropriate antidiuresis. *N. Engl. J. Med.* **356**, 2064–2072 (2007).
2. Waikar, S. S., Mount, D. B. & Curhan, G. C. Mortality after hospitalization with mild, moderate, and severe hyponatremia. *Am. J. Med.* **122**, 857–865 (2009).
3. Kim, W. R. *et al.* Hyponatremia and mortality among patients on the liver-transplant waiting list. *N. Engl. J. Med.* **359**, 1018–1026 (2008).
4. Gheorghiade, M. *et al.* Characterization and prognostic value of persistent hyponatremia in patients with severe heart failure in the ESCAPE Trial. *Arch. Intern. Med.* **167**, 1998–2005 (2007).
5. Kovesdy, C. P. *et al.* Hyponatremia, hypernatremia, and mortality in patients with chronic kidney disease with and without congestive heart failure. *Circulation* **125**, 677–684 (2012).
6. Nielsen, S. *et al.* Vasopressin increases water permeability of kidney collecting duct by inducing translocation of aquaporin-CD water channels to plasma membrane. *Proc. Natl. Acad. Sci. U.S.A.* **92**, 1013–1017 (1995).
7. Miyazaki, T. *et al.* Therapeutic Effects of Tolvaptan, a Potent, Selective Nonpeptide Vasopressin V2 Receptor Antagonist, in Rats with Acute and Chronic Severe Hyponatremia. *Endocrinology* **146**, 3037–3043 (2005).
8. Schrier, R. W. *et al.* Tolvaptan, a selective oral vasopressin V2-receptor antagonist, for hyponatremia. *N. Engl. J. Med.* **355**, 2099–2112 (2006).
9. Verbalis, J. G. *et al.* Efficacy and safety of oral tolvaptan therapy in patients with the syndrome of inappropriate antidiuretic hormone secretion. *Eur. J. Endocrinol.* **164**, 725–732 (2011).
10. Udelson, J. E. *et al.* A multicenter, randomized, double-blind, placebo-controlled study of tolvaptan monotherapy compared to furosemide and the combination of tolvaptan and furosemide in patients with heart failure and systolic dysfunction. *J. Card. Fail.* **17**, 973–981 (2011).
11. Boertien, W. E. *et al.* Short-term Effects of Tolvaptan in Individuals With Autosomal Dominant Polycystic Kidney Disease at Various Levels of Kidney Function. *Am. J. Kidney Dis.* **65**, 833–841 (2015).
12. Bhandari, S. *et al.* A systematic review of known interventions for the treatment of chronic nonhypovolaemic hypotonic hyponatraemia and a meta-analysis of the vaptans. *Clin. Endocrinol. (Oxf)* **86**, 761–771 (2017).
13. Sterns, R. H., Riggs, J. E. & Schochet, S. S. Osmotic demyelination syndrome following correction of hyponatremia. *N. Engl. J. Med.* **314**, 1535–1542 (1986).
14. Sterns, R. H., Silver, S., Kleinschmidt-DeMasters, B. K. & Rojiani, A. M. Current perspectives in the management of hyponatremia: prevention of CPM. *Expert Rev Neurother* **7**, 1791–1797 (2007).
15. Torres, V. E. *et al.* Tolvaptan in patients with autosomal dominant polycystic kidney disease. *N. Engl. J. Med.* **367**, 2407–2418 (2012).
16. Torres, V. E. *et al.* Tolvaptan in Later-Stage Autosomal Dominant Polycystic Kidney Disease. *N. Engl. J. Med.* **377**, 1930–1942 (2017).
17. Wu, Y. *et al.* Mechanisms of tolvaptan-induced toxicity in HepG2 cells. *Biochem. Pharmacol.* **95**, 324–336 (2015).
18. O'Dowd, B. F. *et al.* A human gene that shows identity with the gene encoding the

772 angiotensin receptor is located on chromosome 11. *Gene* **136**, 355–360 (1993).
773 19. Tatemoto, K. *et al.* Isolation and characterization of a novel endogenous peptide ligand
774 for the human APJ receptor. *Biochem. Biophys. Res. Commun.* **251**, 471–476 (1998).
775 20. De Mota, N. *et al.* Apelin, a potent diuretic neuropeptide counteracting vasopressin
776 actions through inhibition of vasopressin neuron activity and vasopressin release. *Proc. Natl.*
777 *Acad. Sci. U.S.A.* **101**, 10464–10469 (2004).
778 21. Azizi, M. *et al.* Reciprocal regulation of plasma apelin and vasopressin by osmotic
779 stimuli. *J. Am. Soc. Nephrol.* **19**, 1015–1024 (2008).
780 22. Gerbier, R. *et al.* Development of original metabolically stable apelin-17 analogs with
781 diuretic and cardiovascular effects. *FASEB J.* **31**, 687–700 (2017).
782 23. Iturrioz, X. *et al.* By Interacting with the C-terminal Phe of Apelin, Phe(255) and
783 Trp(259) in Helix VI of the Apelin Receptor Are Critical for Internalization. *J. Biol. Chem.* **285**,
784 32627–32637 (2010).
785 24. Reaux, A. *et al.* Physiological role of a novel neuropeptide, apelin, and its receptor in the
786 rat brain. *J. Neurochem.* **77**, 1085–1096 (2001).
787 25. Reaux, A., Gallatz, K., Palkovits, M. & Llorens-Cortes, C. Distribution of apelin-
788 synthesizing neurons in the adult rat brain. *Neuroscience* **113**, 653–662 (2002).
789 26. O'Carroll, A. M., Selby, T. L., Palkovits, M. & Lolait, S. J. Distribution of mRNA
790 encoding B78/apj, the rat homologue of the human APJ receptor, and its endogenous ligand
791 apelin in brain and peripheral tissues. *Biochim. Biophys. Acta* **1492**, 72–80 (2000).
792 27. Hus-Citharel, A. *et al.* Effect of apelin on glomerular hemodynamic function in the rat
793 kidney. *Kidney International* **74**, 486–494 (2008).
794 28. Hus-Citharel, A. *et al.* Apelin Counteracts Vasopressin-Induced Water Reabsorption via
795 Cross Talk Between Apelin and Vasopressin Receptor Signaling Pathways in the Rat Collecting
796 Duct. *Endocrinology* **155**, 4483–4493 (2014).
797 29. Boulkeroua, C. *et al.* Apelin-13 Regulates Vasopressin-Induced Aquaporin-2 Expression
798 and Trafficking in Kidney Collecting Duct Cells. *Cell. Physiol. Biochem.* **53**, 687–700 (2019).
799 30. Galanth, C., Hus-Citharel, A., Li, B. & Llorens-Cortès, C. Apelin in the control of body
800 fluid homeostasis and cardiovascular functions. *Curr. Pharm. Des.* **18**, 789–798 (2012).
801 31. Flahault, A., Couvineau, P., Alvear-Perez, R., Iturrioz, X. & Llorens-Cortes, C. Role of
802 the Vasopressin/Apelin Balance and Potential Use of Metabolically Stable Apelin Analogs in
803 Water Metabolism Disorders. *Front Endocrinol (Lausanne)* **8**, 120 (2017).
804 32. Reaux, A., Morinville, A., Burlet, A., Llorens-Cortes, C. & Beaudet, A. Dehydration-
805 Induced Cross-Regulation of Apelin and Vasopressin Immunoreactivity Levels in Magnocellular
806 Hypothalamic Neurons. *Endocrinology* **145**, 4392–4400 (2004).
807 33. Blanchard, A. *et al.* An abnormal apelin/vasopressin balance may contribute to water
808 retention in patients with the syndrome of inappropriate antidiuretic hormone (SIADH) and heart
809 failure. *J. Clin. Endocrinol. Metab.* **98**, 2084–2089 (2013).
810 34. Hasler, U. *et al.* Long term regulation of aquaporin-2 expression in vasopressin-
811 responsive renal collecting duct principal cells. *J. Biol. Chem.* **277**, 10379–10386 (2002).
812 35. Bens, M., Chassin, C. & Vandewalle, A. Regulation of NaCl transport in the renal
813 collecting duct: lessons from cultured cells. *Pflugers Arch.* **453**, 133–146 (2006).
814 36. Chassin, C. *et al.* Pore-forming epsilon toxin causes membrane permeabilization and
815 rapid ATP depletion-mediated cell death in renal collecting duct cells. *Am. J. Physiol. Renal*
816 *Physiol.* **293**, F927-937 (2007).
817 37. Le Bouffant, F., Hus-Citharel, A. & Morel, F. Metabolic CO2 production by isolated

single pieces of rat distal nephron segments. *Pflugers Arch.* **401**, 346–353 (1984).
38. Boitard, S. E. *et al.* Brain renin-angiotensin system blockade with orally active aminopeptidase A inhibitor prevents cardiac dysfunction after myocardial infarction in mice. *J. Mol. Cell. Cardiol.* **127**, 215–222 (2019).
39. Team, R. C. *R: A language and environment for statistical computing. R Foundation for Statistical Computing, Vienna, Austria. 2018*.
40. El Messari, S. *et al.* Functional dissociation of apelin receptor signaling and endocytosis: implications for the effects of apelin on arterial blood pressure. *J. Neurochem.* **90**, 1290–1301 (2004).
41. Reck, F. *et al.* Novel N-linked aminopiperidine inhibitors of bacterial topoisomerase type II: broad-spectrum antibacterial agents with reduced hERG activity. *J. Med. Chem.* **54**, 7834–7847 (2011).
42. Taheri, S. *et al.* The effects of centrally administered apelin-13 on food intake, water intake and pituitary hormone release in rats. *Biochem. Biophys. Res. Commun.* **291**, 1208–1212 (2002).
43. Urwyler, S. A. *et al.* Plasma Apelin concentrations in Patients with Polyuria-Polydipsia Syndrome. *J. Clin. Endocrinol. Metab.* jc20161158 (2016) doi:10.1210/jc.2016-1158.
44. Dai, L., Smith, P. M., Kuksis, M. & Ferguson, A. V. Apelin acts in the subfornical organ to influence neuronal excitability and cardiovascular function. *J. Physiol. (Lond.)* **591**, 3421–3432 (2013).
45. Hindmarch, C. *et al.* Microarray analysis of the transcriptome of the subfornical organ in the rat: regulation by fluid and food deprivation. *Am. J. Physiol. Regul. Integr. Comp. Physiol.* **295**, R1914-1920 (2008).
46. Tatemoto, K. *et al.* The novel peptide apelin lowers blood pressure via a nitric oxide-dependent mechanism. *Regul. Pept.* **99**, 87–92 (2001).
47. Japp, A. G. *et al.* Acute cardiovascular effects of apelin in humans: potential role in patients with chronic heart failure. *Circulation* **121**, 1818–1827 (2010).
48. Dray, C. *et al.* Apelin stimulates glucose utilization in normal and obese insulin-resistant mice. *Cell Metab.* **8**, 437–445 (2008).
49. Lacquaniti, A. *et al.* Apelin and copeptin: two opposite biomarkers associated with kidney function decline and cyst growth in autosomal dominant polycystic kidney disease. *Peptides* **49**, 1–8 (2013).